Proceedings of ICAPP '06
Reno, NV USA, June 4-8, 2006
Paper 6312

Comparative Transient Analysis of a Gas-cooled Fast Reactor for Different Fuel Types

P. Petkevich*, K. Mikityuk[+], P. Coddington, S. Pelloni, R. Chawla[*]
Laboratory for Reactor Physics and Systems Behaviour
Paul Scherrer Institute, CH-5232 Villigen PSI, Switzerland
[*]*Co-affiliation: Ecole Polytechnique Fédérale de Lausanne (EPFL)*
CH-1015 Lausanne, Switzerland
[+]*Tel: +41 56 310 2385 , Fax: +41 56 310 2327 , Email: konstantin.mikityuk@psi.ch*

Abstract – *Several new fuel designs are currently being considered for the Generation-IV gas-cooled fast reactor. Two designs have been analysed in the paper: 1) a ceramic honeycomb plate matrix containing fuel cylinders (slab geometry) and 2) a pin with fuel pellets in a ceramic cladding (rod geometry). Mixed uranium-plutonium carbide is the fuel in both cases, while the matrix/cladding material is silicon carbide. A simplified approach to the transient simulation of the heterogeneous plate design has been developed and benchmarked against detailed finite-element code calculations. The limits of applicability of the simplified approach to transient calculations have been estimated and directions for its further improvement have been formulated. The slab and rod fuel designs were then compared from the viewpoint of their thermal transient response to a number of hypothetical accidents, including loss of heat sink, core overcooling, loss of flow and transient overpower.*

I. INTRODUCTION

The 2400 MWt helium-cooled (U-Pu)C-fuelled fast reactor [1] is one of the most promising Generation-IV concepts [2]. The design goal of the Gas-cooled Fast Reactor (GCFR) is to combine a number of features, including flexible breeding parameters and high coolant temperatures, allowing for both high thermo-dynamic efficiency and hydrogen production. The GCFR core design is still under development; in particular, several options for the fuel design are being considered currently [3]. The purpose of the work presented here is to compare two fuel designs (with slab and rod geometries, respectively) from the viewpoint of their thermal response to a number of different transient types. In common with most such analysis, the fuel element geometry is assumed to remain unchanged during the transients considered.

In the above context, the methodology for a simplified simulation of the highly heterogeneous GCFR plate-type fuel element has been developed and benchmarked against detailed steady-state and transient calculations with a state-of-the-art finite-element code [4]. As the latter calculations are time-consuming, they are not used for the comprehensive safety analysis itself, but only for benchmarking purposes. Thereby, the limits of applicability of the simplified approach to transient calculations have been estimated, and directions are outlined for its further improvement.

II. FUEL DESIGNS

As mentioned, the two options considered for the GCFR fuel elements are of plate (slab) and rod designs (Fig.1).

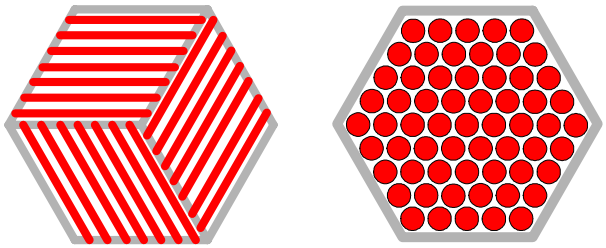

Fig.1. Fuel assembly design of a) slab and b) rod geometry.

In both cases, the fuel is mixed uranium-plutonium carbide and the structural material is silicon carbide. The plate fuel element is a SiC honeycomb structure containing cylindrical fuel pellets and covered by flat SiC cladding from both sides (Fig.2). The fuel assembly contains 21 plates arranged as shown in Fig.1a. The plate thickness is 7 mm. The fuel rod design (Fig.1b) is more traditional and consists of a stack of the cylindrical fuel pellets within a SiC cladding tube. The outer diameter of the fuel pin is 9.7 mm. In this case, the fuel assembly consists of 217 fuel rods. This number was chosen to have the mass of fuel and

structural materials as close as possible in the two options. The various other reactor parameters were kept the same for the two cases (see [1] for a detailed specification). In particular, the coolant temperatures at core inlet/outlet were 480/850ºC.

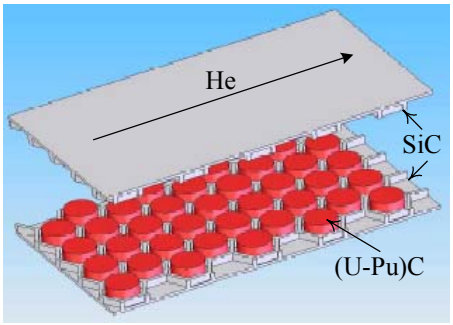

Fig.2. Schematics of the plate fuel element design.

II. SIMULATION: CODES AND ASSUMPTIONS

The TRAC/AAA code [5], which forms part of the PSI FAST code system [6], has been specially adapted for the transient analysis of advanced fast reactors and used here for the comparative study for the two fuel types. In order to perform the present analysis, the code material property data base was extended to cover new materials, including mixed uranium-plutonium carbide and silicon carbide. The reactor core was represented in TRAC/AAA as two zones, with peaking factors taken from the neutronic calculations and a hot fuel assembly with a 15% peaking factor. The TRAC/AAA nodalization used is shown in Fig.3.

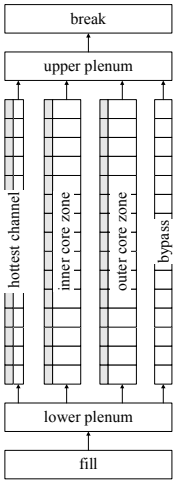

Fig.3. TRAC/AAA nodalization diagram.

The inlet flow resistance of the two core zones was adjusted to flatten the coolant outlet temperature. The resistance of the hot assembly was left unchanged. The TRAC/AAA point kinetics model with reactivity feedbacks was used for the calculations.

The ERANOS (Version 2) code system [7,8,9] has been used to perform the steady-state neutronic calculations necessary for the transient analysis, viz. the spatial power distribution, the neutron kinetics parameters, reactivity coefficients, etc. More specifically, ECCO calculations, ECCO being the lattice code of ERANOS, were performed for homogeneous configurations to generate self-shielded cross-sections in 33 broad energy groups. Thereby, the available adjusted JEF-2.2 data library, ERALIB-1, was used. Forward and adjoint flux calculations were then carried out using the two-dimensional discrete-ordinates transport-theory code BISTRO in conjunction with the 33 broad group cross-sections and P_1S_8-approximations. The reactor geometry was simulated using a detailed 2D cylindrical core model. Core-average reactivity effects were assessed by means of additional forward calculations for modified core conditions. These include reactivity variations as a result of homogeneous changes of the fuel temperature or of coolant density, as well as those originating from thermal-mechanical expansion of the core in both the radial and axial direction (under the main assumption that the fuel mass is preserved). The kinetics parameters for use in TRAC/AAA were determined by applying linear perturbation theory. The various ERANOS results are presented in Table I. It should be noted that, since the volume fractions of the core materials in the two designs are very close, the reactivity coefficients can be assumed to be the same for the plate and rod options.

TABLE I

GCFR reactivity coefficients and kinetics parameters

Doppler constant*, pcm**	-1917
Coolant temperature, $\Delta(1/k_{eff})$/K	$7.216/T^{2***}$
Core radial expansion, pcm/K	-0.251
Core axial expansion, pcm/K	-0.027
β_{eff}, pcm	399
Λ, μs	1.35

*Reactivity effect assumed to be a logarithmic function of fuel temperature: $\Delta\rho(T_0 \rightarrow T) = K_D \ln(T/T_0)$, where K_D is the Doppler constant

**1 pcm = 10^{-5} $\Delta(1/k_{eff})$

***T is the temperature, K

In this study, we did not analyse loss-of-coolant accidents due to reactor depressurisation, so that the transient coolant density change can be assumed to result from temperature variation only. As the constant reactivity coefficient calculated by ERANOS is the derivative of reactivity with respect to the gas density, it was converted to the temperature coefficient required by TRAC/AAA as follows:

$$\frac{\partial \rho}{\partial T} = \frac{\partial \rho}{\partial \gamma}\frac{\partial \gamma}{\partial T} = -\frac{pM}{2RT^2}\frac{\partial \rho}{\partial \gamma} \quad (1)$$

where ρ is the reactivity (Δk/k), T the temperature (K), γ the gas density (kg/m^3), p the gas pressure (Pa), M the gas molar mass (mol/kg) and R = 8.31 J/kg-K.

Thus, as seen from Table I, significant features of the GCFR core are that the coolant temperature coefficient is positive and reduces with temperature as $1/T^2$, and that the magnitude of the Doppler constant is considerably greater than in a fast-spectrum core with oxide fuel and stainless steel cladding [10,11,12], mainly because of softer neutron spectrum caused by the carbon-based matrix material leading to enhanced U-238 resonance capture.

The core radial expansion coefficient is about ten times higher than the axial expansion coefficient (see Table I). It can be explained by the fact that the core radial expansion is controlled by the steel diagrid expansion, while the axial one – by the silicon carbide matrix expansion. The thermal expansion coefficient of steel is by a factor of three higher than this coefficient for silicon carbide. It means that the temperature increase by 1 degree results in three times higher increase in core radius than in the core height. Moreover, the 1%-change of the diagrid size means much higher change in the core top and bottom surface (and hence the axial leakage) compared to the change in the lateral core surface (and hence the radial leakage) when the core height increases by 1%.

As the TRAC/AAA code is not designed to simulate heterogeneous structures such as the plate-type fuel element (see Fig.2 and Fig.4a), approximations should be made. The simplified approach adopted currently involves homogenization of the fuel pellets with the inner part of the honeycomb structure, i.e. with the ceramic walls between the pellets (Fig.4b).

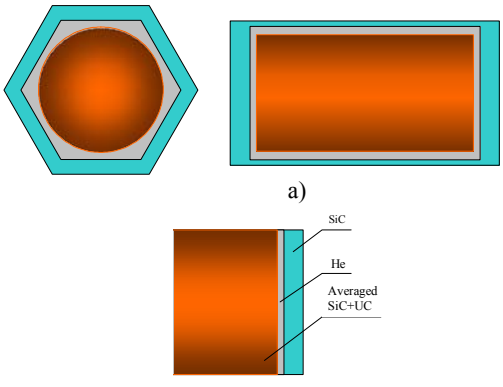

Fig.4. Schematics of a) a single cell of the plate fuel element design and b) simplified model for the TRAC/AAA calculations.

The following guidelines were used to calculate the properties of the homogenized material:

- thermal conductivity of the homogenized material is assumed equal to that of pure fuel;
- density of the homogenized material is calculated as the total mass of fuel and structures divided by their total volume;
- specific heat of the homogenized material is calculated as the total heat capacity (J/ºC) of fuel and structures divided by their total mass.

To check the validity of the above simplifications, i.e. to estimate the error introduced by the homogenization, the ANSYS finite-element code [4] was used to develop a detailed model for 1/12th of the plate fuel element cell, i.e. the minimal representative sector. The geometry modelled for the ANSYS calculations is given in Fig.5. Boundary conditions on the surface A'B'C' were modelled by means of the bulk helium temperature and heat exchange coefficient, both taken from the TRAC/AAA calculations, while zero heat flux was assumed for all other surfaces. The time history for the power density was also taken from the TRAC/AAA calculations.

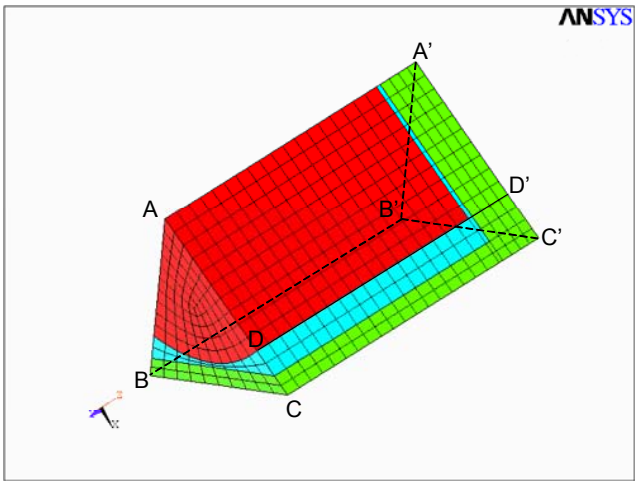

Fig.5. Nodalization scheme of the plate-type fuel element cell for the ANSYS calculations.

For additional verification, a homogeneous ANSYS model, completely analogous to the TRAC/AAA model (Fig.4b), was also developed. A heterogeneous ANSYS model was not developed for the fuel rod option, as the TRAC code was originally developed for LWRs and hence already extensively verified for fuel pins with cylindrical geometry.

III. STEADY STATE

The steady-state axial fuel and clad temperature profiles in the central fuel assembly calculated by TRAC/AAA for the two fuel designs are presented in Fig.6.

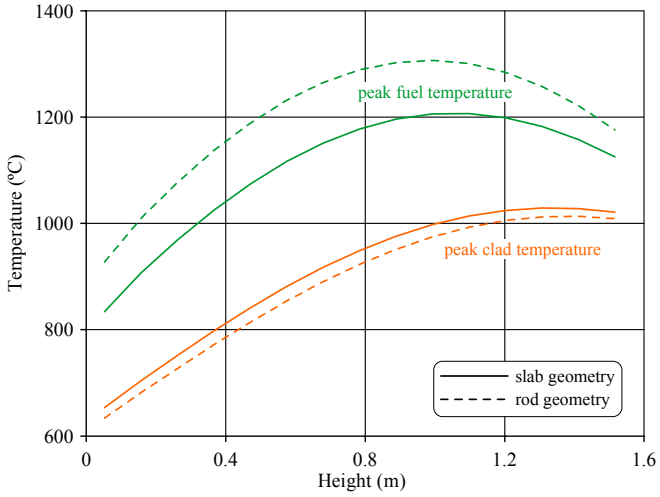

Fig.6. Steady-state axial fuel and clad temperature profiles in the central fuel assembly calculated by the TRAC/AAA code for the slab and rod fuel geometries.

The difference between the two options in the peak fuel and clad temperatures are 100ºC and 15ºC, respectively. The fuel temperature is higher in the rod design (because the fuel thermal resistance is higher in the rod compared to the plate) and the clad temperature is higher in the plate design (because the rods have higher heat exchange area compared to the plates).

As already mentioned, the heterogeneous plate design is beyond the scope of the original TRAC/AAA application area. Accordingly, the TRAC/AAA results were checked against the detailed geometry ANSYS model (see Fig.5). The steady-state fuel and clad temperature profiles along the axis of the peak-power fuel pellet in the central fuel assembly with the plate-type fuel elements, as calculated by the ANSYS and TRAC/AAA codes, are presented in Fig.7a.

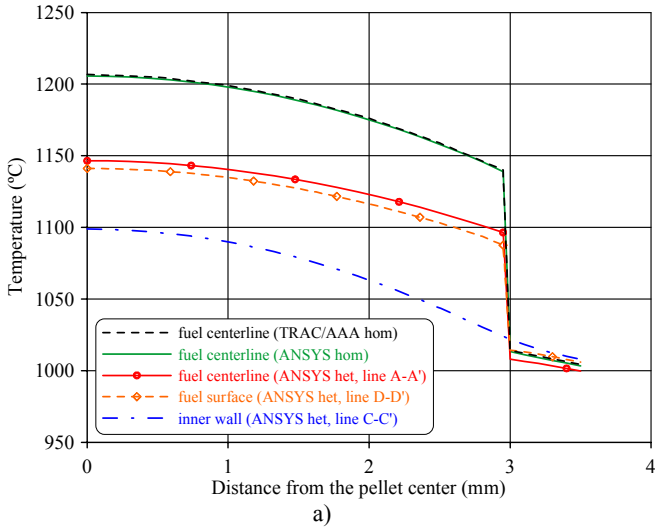

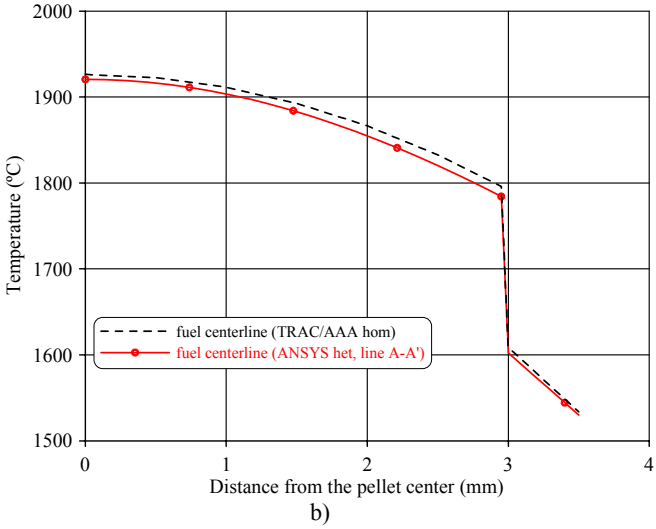

Fig.7. Steady-state fuel and clad temperature profiles along the peak-power fuel pellet axis calculated by the ANSYS and TRAC/AAA codes (see Fig.5): a) for nominal power; b) for two-fold power.

It can be seen from this figure that the difference in the peak fuel temperatures between the heterogeneous (ANSYS) and homogeneous (TRAC/AAA) models is quite significant, viz. 60ºC. This discrepancy can be explained by the facts that the fuel-to-clad heat exchange area and the effective gap size are greater in the heterogeneous model compared to the homogeneous case, while the clad-to-coolant heat exchange area is the same. It should be noted that the discrepancy between the ANSYS and TRAC/AAA code predictions (see Fig.7a) is a complex function of the power level. For instance, this discrepancy reduces to almost zero for the case of 200% power (see Fig.7b).

The inner ceramic wall, which is a very good heat conductor, is explicitly simulated in the heterogeneous ANSYS model. At the nominal power, the heat transfer through the lateral surface of the fuel pellet makes the steady-state fuel cooling more effective. Thus, the steady-state fuel temperature at the nominal power is estimated conservatively in the homogeneous model. The almost identical results of ANSYS and TRAC/AAA for the homogeneous model (Fig.7a) demonstrate the consistency of the simplified-geometry predictions with the two codes.

The steady-state clad temperature and heat flux profiles on the clad surface (along axis A'C' in Fig.5) calculated by the ANSYS code is shown in Fig.8. It can be seen from the figure that the peak clad temperature and heat flux are not in the region of the fuel pellet, but in the area of the inner wall.

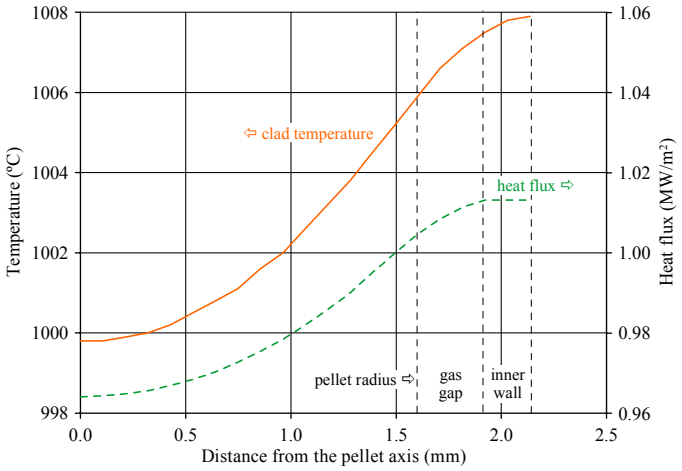

Fig.8. Steady-state clad temperature and heat flux profiles on the clad surface (along axis A'C' in Fig.5) calculated by the ANSYS code for nominal power.

IV. TRANSIENT ANALYSIS

The behaviour of the GCFR core has been analyzed for a number of hypothetical accidents, with and without scram (protected and unprotected). The calculations were performed with the TRAC/AAA code using point kinetics.

The following reactivity feedbacks were simulated (see Table I for values):

- the Doppler effect under the assumption of a logarithmic dependence of reactivity on the fuel temperature;
- reactivity change caused by a change of the effective core height due to the fuel/structure thermal expansion under assumption of the absence of pellet-clad mechanical interaction;
- reactivity change caused by the change in the core effective radius due to thermal expansion of the core diagrid (or other support structure);
- reactivity change caused by the change in the effective coolant density in the core to account for coolant thermal expansion.

The following accidents were considered:

- unprotected core overheating (loss of heat sink, LOHS), simulated by increasing the inlet coolant temperature by 100ºC;
- unprotected core overcooling (OVC), simulated by reducing the inlet coolant temperature by 100ºC;
- protected and unprotected loss of flow accident (LOF), simulated by reducing the gas flowrate with a rundown time of 30 s and a natural circulation level of 2% of the nominal value;
- protected and unprotected transient overpower (TOP), simulated by inserting a positive reactivity of 1.0 $ over a second.

The scram (-3 $ inserted over 2 s) was assumed to be actuated when the average coolant temperature at the core outlet increases up to 920ºC, i.e. by ~20% of the nominal coolant heating in the core.

IV.A. Loss of heat sink (LOHS) accident

The LOHS accident was calculated to examine the response of the GCFR core to an increase of the inlet coolant temperature. Only the unprotected (ULOHS) accident was considered. The response of the core can be seen in Fig.9-Fig.11. The increase of the coolant temperature at the core inlet leads to a decrease of the average core coolant density and to the introduction of positive reactivity (see the reactivity balance in Fig.10). As a consequence, the reactor power (Fig.9) and core temperatures (Fig.11) start to increase. The increase in the fuel temperature leads to negative reactivity insertion which counterbalances the coolant density effect. As a result, the reactivity and the reactor power decrease. The power first increases in both designs by about 6% and finally stabilizes at about 90% of the nominal value. The peak fuel/cladding temperatures in the ULOHS accident are 1270/1100ºC for the plate design and 1380/1100ºC for the rod design (see Fig.11).

IV.B. Core overcooling (OVC) accident

The OVC accident was calculated to determine the response of the GCFR core to a decrease of the inlet coolant temperature. Only the unprotected accident (UOVC) was considered. The response of the core can be seen in Fig.12-Fig.14. The decrease in the coolant temperature at the core inlet leads to an increase of the average core coolant density and to a reactivity decrease (see the reactivity balance in Fig.13). As a consequence, the reactor power (Fig.12) and core temperatures (Fig.14) start to diminish. The decrease in the fuel temperature leads to a positive reactivity insertion which counterbalances the coolant density effect. As a result the reactivity and the reactor power increase. The power decreases in both designs by about 6% and finally stabilizes at about 105 to 110% of the nominal value. The fuel/cladding temperatures in the considered UOVC accident do not exceed the steady-state values at any stage (see Fig.14).

It is thus seen that, in general, the core shows good self-protection behaviour against perturbations of the core inlet coolant temperature. The increase/decrease of the inlet temperature by 100ºC leads to the decrease/increase of the core power and flowrate by about 10%, while asymptotic fuel temperatures remain almost the same as under nominal conditions.

IV.C. Loss of flow (LOF) accident

The LOF accident was calculated to examine the response of the GCFR core to a reduction of the coolant flowrate. Fig.15-Fig.17 show the TRAC/AAA results for the protected case (PLOF), and Fig.18-Fig.20 those for the unprotected (ULOF) accident. The core mass flowrate was specified as a boundary condition: it was assumed to reduce by a factor of 2 every 30 s, while the asymptotic value (the natural circulation level) was set to be 2% of the nominal value (see the flowrate curve in Fig.15). These assumptions will be reviewed following transient analysis studies for the whole system.

The loss of flow leads to a deterioration of the heat removal, thus causing increases of the fuel, cladding and coolant temperatures. The reactivity balances are shown in Fig.16 and Fig.19 for the cases with and without scram, respectively. The fuel heat-up leads to the insertion of negative reactivity and a reduction of the core power.

The scram signal for the PLOF transient occurs at about 12 s, reducing the reactor power to the decay heat level. After the scram initiation, the temperature falls rapidly during 30-35 seconds, reaching values below the operating level. The peak fuel/cladding temperatures in the PLOF accident are 1270/1130ºC for the plate design and 1360/1110ºC for the rod design (see Fig.17).

In the ULOF case, the negative reactivity effect of the fuel temperature change reduces the core power to 8.6% of the nominal value for the plate design and 10.8% for the rod design (see Fig.19). The peak fuel/cladding temperatures in this accident are 1600/1610ºC for the plate design and 1730/1780ºC for the rod design (see Fig.18). After about 100 s, the peak clad temperature becomes higher than the fuel temperature. This can be explained by the fact that the fuel temperature axial profile, i.e. the axial position of the peak fuel temperature changes. However, the difference is not very significant, the peak fuel temperature being in fact very close to the peak clad temperature.

IV.D. Transient overpower (TOP) accident

The TOP accident was calculated to determine the response of the GCFR core to a reactivity insertion. The case considered is the insertion of a reactivity of 1 dollar over 1 second. The response of the core can be seen in Fig.21-Fig.23 for the protected case (PTOP) and in Fig.24-Fig.26 for the unprotected accident (UTOP). The reactor power increases to 650% and 535% for the plate and rod designs, respectively. Due to the very rapid reactor power escalation, the scram was actuated in less than 1.5 s after transient initiation (Fig.21), reducing the power to the decay heat level. In the UTOP case, the power also reduces, but due to reactivity feedbacks caused by the fuel heating. The fuel temperature reactivity feedback is sufficiently strong to lead to a stabilization of the power at ~200% of the nominal value (see Fig.24). The reactivity balances are shown in Fig.22 and Fig.25 for the cases with and without scram, respectively.

The peak fuel/clad temperatures in the PTOP accident are 1500/1260ºC for the plate design, and 1670/1225ºC for the rod design (see Fig.23). Maximal temperatures of the components are obtained within the first 5 seconds of the transient, having a pronounced peak at about 2 seconds (especially for reactor power). After that, all the parameters decrease monotonously to values below the operating level.

The peak fuel/clad temperatures in the UTOP accident are 2085/1770ºC for the plate design, and 2235/1740ºC for the rod design (see Fig.26). The peak temperatures stay well below the melting points of the carbide fuel (2500ºC) and SiC cladding (2830ºC).

IV.E. Homogeneous versus heterogeneous geometry comparison for TOP accident

For the case of the UTOP, a transient thermal analysis of the plate "hot pellet" was carried out with the ANSYS code, with a detailed 3D representation of the plate-type fuel element. Time-dependent boundary conditions from the TRAC/AAA calculation were used for the purpose.

A comparison of the ANSYS results for the peak fuel temperature with those of the full TRAC/AAA modelling (homogenized fuel region) is shown in Fig.27. A good agreement between heterogeneous ANSYS, homogeneous ANSYS and homogeneous TRAC results is obtained. However the quality of the agreement will depend on the relative values of the thermal parameters (conductivity, density, and specific heat) of the matrix and fuel materials.

To improve the predictions of the simple TRAC/AAA model of the plate-type fuel (Fig.4b), the TRAC/AAA heat transfer module will be modified to include a 2D heat conduction solution in cylindrical geometry, to permit heat exchange from the flat side (end) of a cylindrical fuel pellet. In this case, the hexagonal structure of the inner walls (see Fig.4a) would be simulated with an equivalent cylinder. This approach will allow for further development of not only thermal, but also mechanical models for the GCFR composite fuel.

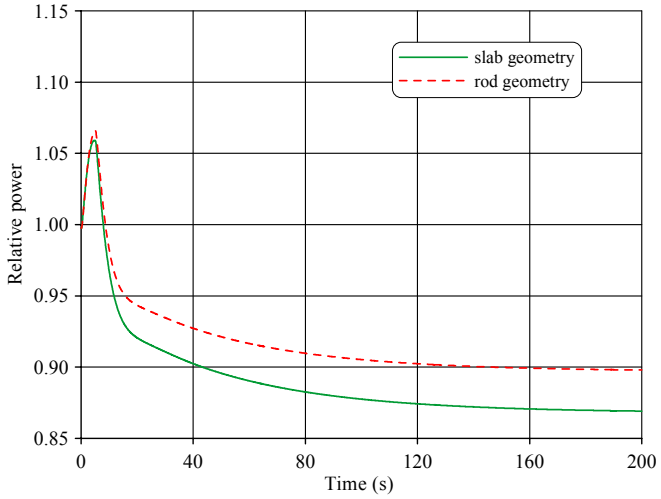

Fig.9. Core power in ULOHS.

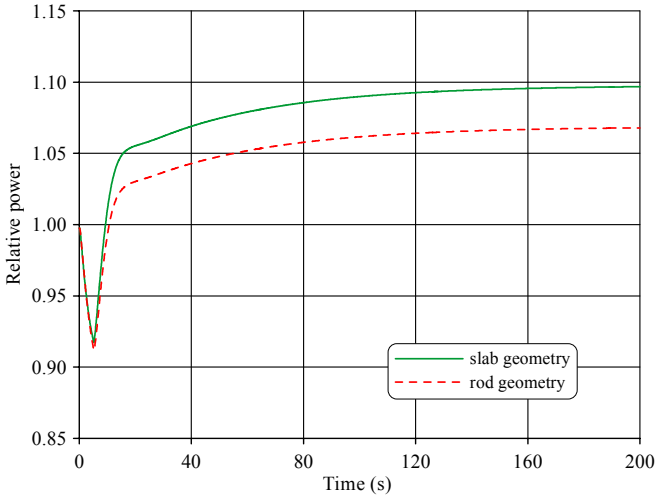

Fig.12. Core power in UOVC.

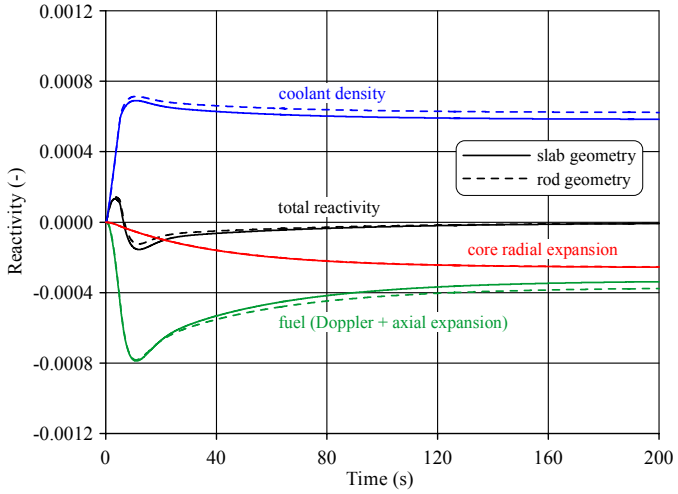

Fig.10. Reactivity components in ULOHS.

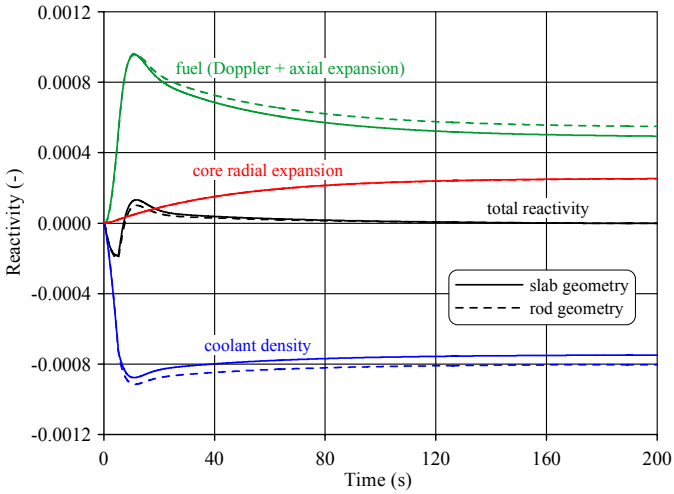

Fig.13. Reactivity components in UOVC.

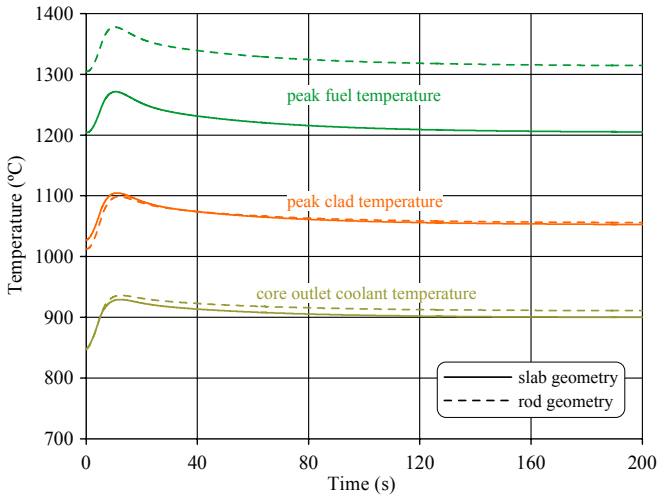

Fig.11. Peak temperatures in ULOHS.

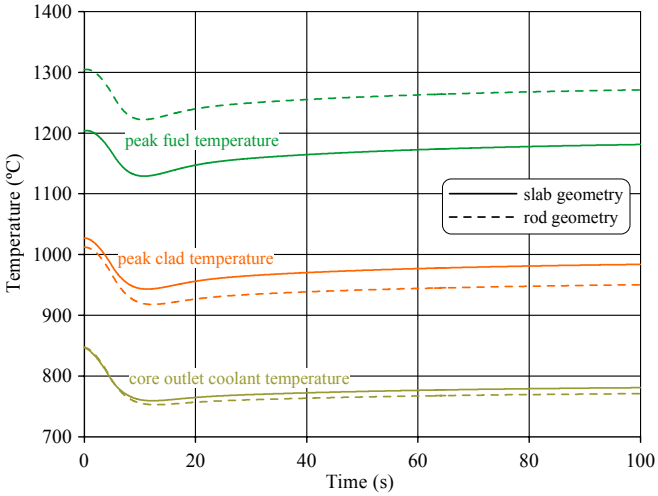

Fig.14. Peak temperatures in UOVC.

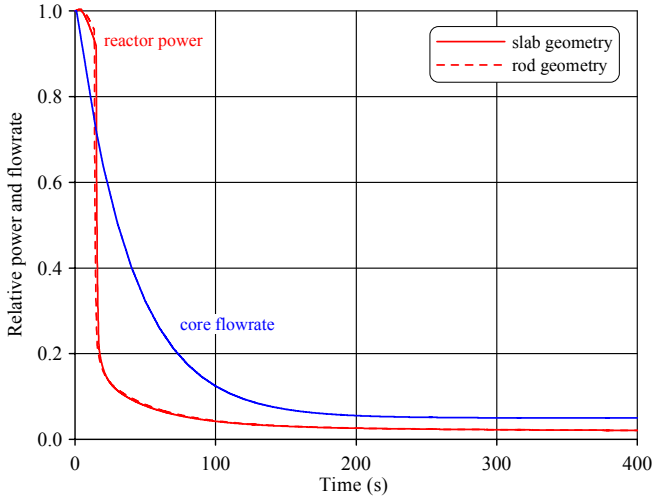

Fig.15. Core power and coolant flowrate in PLOF.

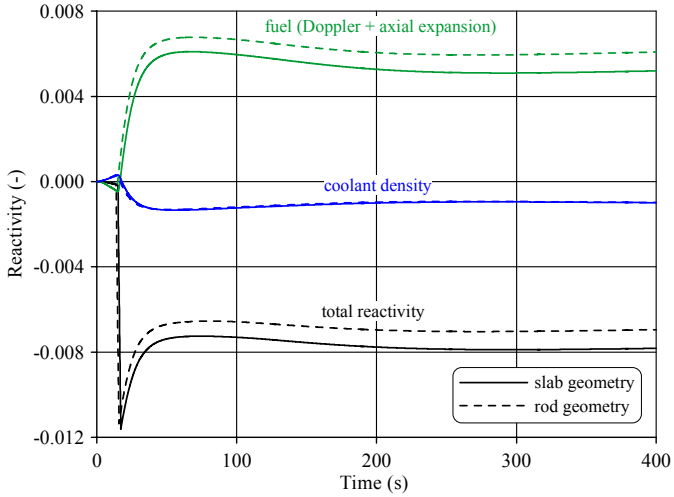

Fig.16. Reactivity components in PLOF.

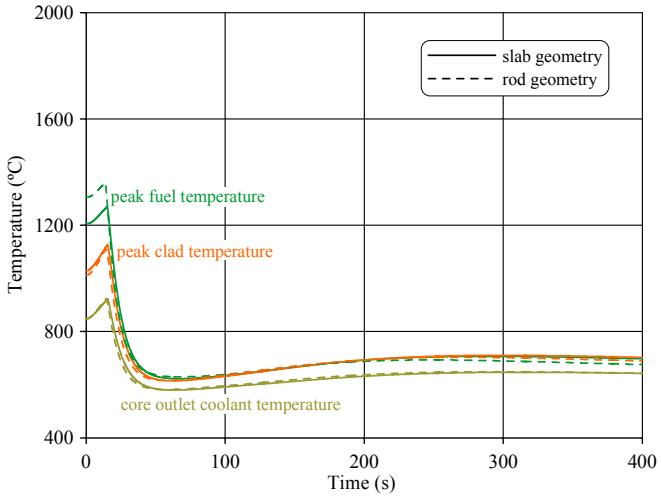

Fig.17. Peak temperatures in PLOF.

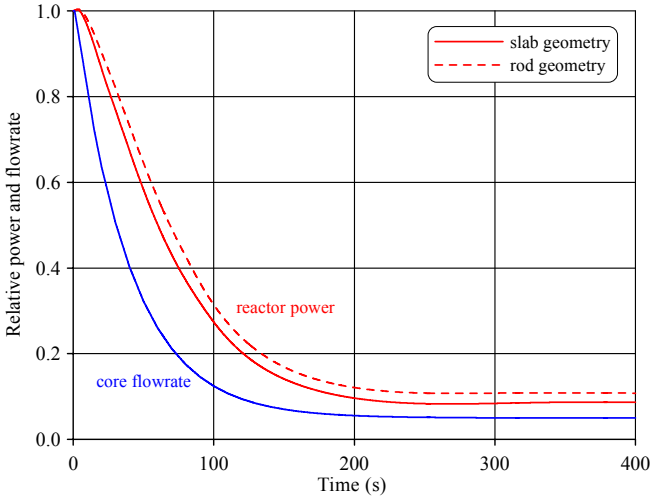

Fig.18. Core power and coolant flowrate in ULOF.

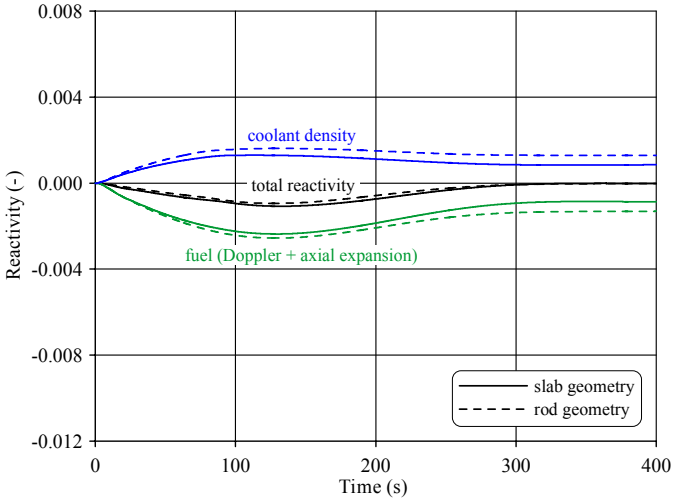

Fig.19. Reactivity components in ULOF.

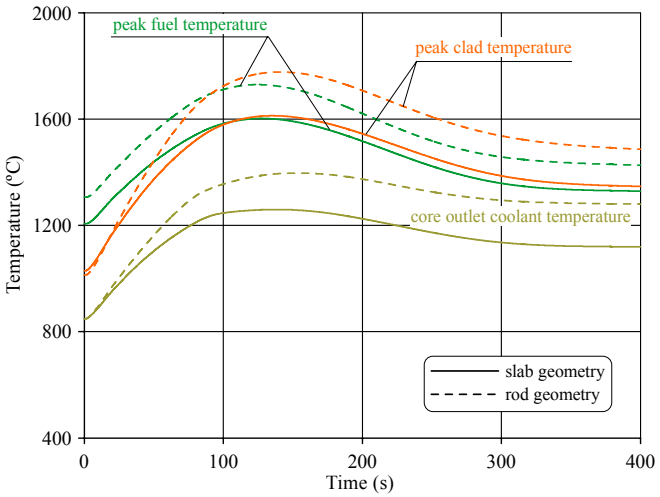

Fig.20. Peak temperatures in ULOF.

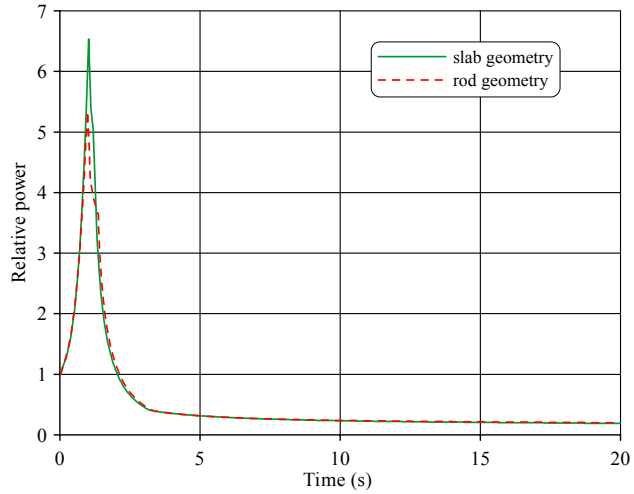

Fig.21. Core power in PTOP.

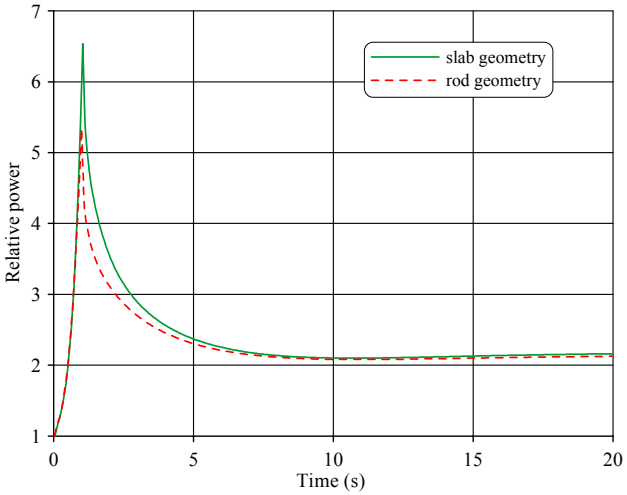

Fig.24. Core power in UTOP.

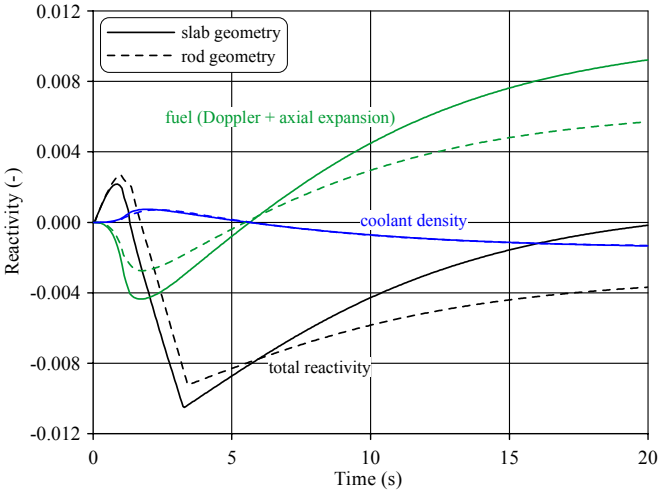

Fig.22. Reactivity components in PTOP.

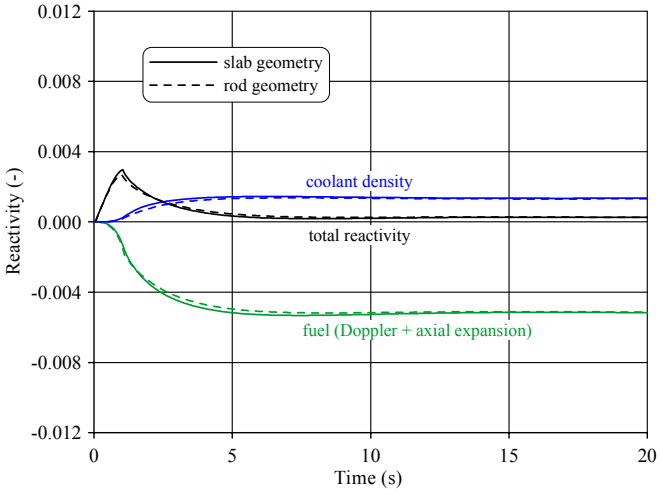

Fig.25. Reactivity components in UTOP.

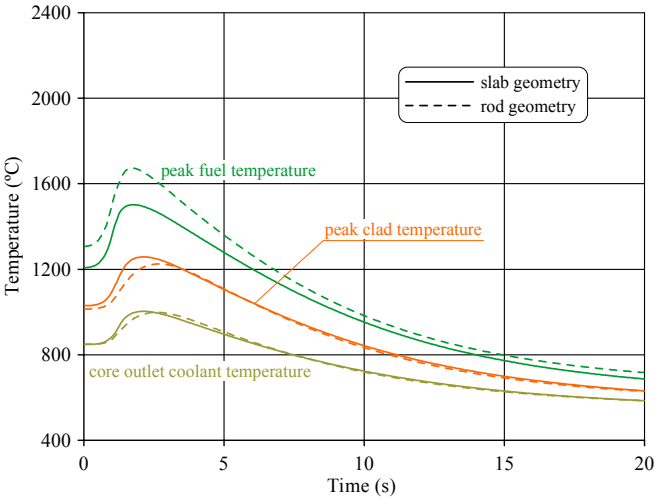

Fig.23. Peak temperatures in PTOP.

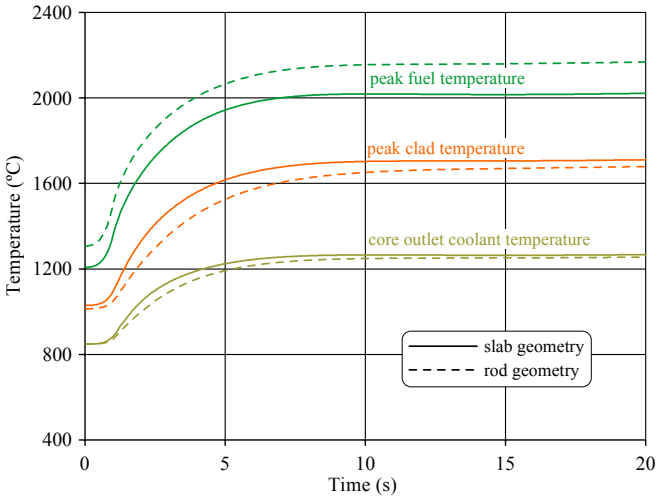

Fig.26. Peak temperatures in UTOP.

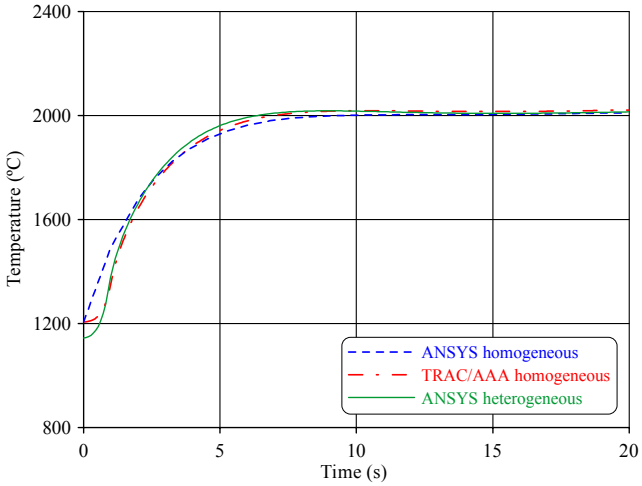

Fig.27. Comparison of TRAC/AAA and ANSYS predictions of peak fuel temperature in plate-type fuel during UTOP (1$ reactivity insertion over 1 s).

V. CONCLUSIONS

Several new fuel designs are currently being considered for the Generation-IV gas-cooled fast reactor, the aim being to increase the exit coolant temperature in order to both improve the thermal efficiency and to provide a basis for hydrogen generation. One of the reference designs is a plate-type fuel element consisting of a ceramic slab-geometry honeycomb matrix containing several-mm diameter fuel cylinders. Another design is for a fuel pin with fuel pellets in a ceramic cladding. Mixed uranium-plutonium carbide is intended to be the fuel in both cases, while the matrix/cladding material is silicon carbide.

A comparative study of the behaviour of the GCFR-2400 core with the slab and rod geometry fuel elements during loss of heat sink, over cooling, loss of flow and transient over power accidents has been performed with the TRAC/AAA code. Both protected (with reactor scram) and unprotected (without scram) regimes were considered.

As the exact modelling of the highly heterogeneous plate structure is impossible with the TRAC/AAA code, a simplified model was developed using smeared thermal-physical properties. The finite-element code ANSYS was used for steady-state thermal analysis of a single fuel cell of the plate-type fuel element. As the calculational time required for the ANSYS FEM model is very high, it could not be used for the comprehensive safety analysis. However, results of this analysis were used to benchmark the simplified fast-running TRAC/AAA model with homogenized material properties. It was found that, in the steady-state regime, the homogenized TRAC/AAA model predicts a peak fuel temperature ~60ºC higher than that predicted by the more detailed heterogeneous ANSYS model, thus making the assessment conservative from this viewpoint.

The peak temperatures reached in the hypothetical accidents simulated with the TRAC/AAA code are presented in Table II.

TABLE II

Peak temperatures of the core components in transients calculated by TRAC/AAA, ºC.

	Plate design			Rod design		
	Fuel	Clad	Coolant (outlet)	Fuel	Clad	Coolant (outlet)
Nominal	1210	1030	850	1310	1015	850
ULOHS	1270	1105	930	1380	1100	940
UOVC	1210	1030	850	1310	1015	850
PLOF	1270	1130	1030	1360	1110	1025
ULOF	1610	1610	1470	1730	1780	1635
PTOP	1500	1260	1130	1670	1225	1120
UTOP	2085	1770	1530	2235	1740	1510

The main difference between the rod and plate-type fuels is that the steady-state peak fuel temperature is ~100ºC higher in the rod design. The difference of the same order in the peak fuel temperature (100-170ºC) is maintained in most of the transients.

The main conclusions of the TRAC/AAA analysis of the various hypothetical accidents are as follows:

1) The GCFR core shows good self-protection against unprotected perturbations of the core inlet coolant temperature (ULOHS and UOVC). The increase (or decrease) of the inlet temperature by 100ºC leads to the decrease (or increase) of the core power and flowrate by about 10%, while the asymptotic fuel temperatures remain almost the same as under nominal conditions.

2) The core protects itself without scram against decrease of the core flowrate. The unprotected reduction of the core inlet coolant flowrate (by a factor of 2 every 30 s and to the natural circulation level of 2% after about 200 s) causes the core to heat up with a consequential decrease of the core power to about 10% of the nominal value due to the high value of the Doppler reactivity feedback. Asymptotically, the peak fuel temperature increases by less than 200ºC, while the clad temperature rises by ~500ºC in the rod design and by ~300ºC in the plate design.

3) The analysis of the fast (1$ within 1 s) reactivity insertion accident shows a good agreement between 3D heterogeneous ANSYS model and simplified homogeneous TRAC model. To improve the predictions of the plate-type fuel the TRAC/AAA heat transfer module will be modified to include a 2D heat conduction solution in cylindrical geometry. In this case, the hexagonal structure of the inner walls would be simulated with an equivalent cylinder. This approach will allow for further development of not only thermal, but also mechanical models for the GCFR composite fuel.

In general, due to the large magnitude of the Doppler constant, the core, with both fuel designs, shows good behaviour for the protected accidents and displays satisfactory self-protection features in the case of unprotected events.

Finally it should be mentioned that, although the melting temperature of SiC (2830ºC) is not exceeded during the considered transients, one should be careful about considering this as the only fuel element failure criterion. The proposed fuel type assumes using SiC reinforced with SiC-fibres (SiCf/SiC) as cladding material. Currently, at least, thermal stability for SiC fibres is provided only till about 1500ºC [13, 14], depending on the fabrication procedure and other factors.

REFERENCES

1. P. MARTIN, N. Chauvin, J.C. Garnier, M. Masson, P. Brossard, P. Anzieu, "Gas Cooled Fast Reactor System: Major Objectives and Options for Reactor, Fuel and Fuel Cycle", *Proceedings of GLOBAL 2005, Paper No. IL002*, Tsukuba, Japan (2005).

2. A Technology Roadmap for Generation IV Nuclear Energy Systems, US DOE Nuclear Energy Research Advisory Committee and the Generation IV International Forum (2002).

3. A. CONTI, A. Ravenet, "Gas cooled Fast Reactors. Fuel Element and Sub-Assembly Concepts", CEA, *Proc. of GFR/ETDR Seminar*, November 2004.

4. ANSYS Basic Analysis Guide, ANSYS Release 9.0, ANSYS, Inc., November 2004.

5. J.W. SPORE, P. Sadasivan and D.R. Liles, "Accelerator Transmutation of Waste Updates for TRAC-M", *LA-UR-01-3660*, June 2001.

6. K. MIKITYUK, S. Pelloni, P. Coddington, E. Bubelis, R. Chawla. "FAST: An advanced code system for fast reactor transient analysis", *Annals of Nuclear Energy*. **32**, 15, 1613-1631 2005.

7. G. RIMPAULT et al., "The ERANOS Data and Code System for Fast Reactor Neutronic Analyses", *Int. Conf. on the New Frontiers of Nuclear Technology: Reactor Physics, Safety and High-Performance Computing, PHYSOR 2002*, Seoul, Korea (2002).

8. G. RIMPAULT, "ERANOS: Manuel des méthodes, le code de cellule ECCO", *Rapport Technique*, CEA, SPRC/LEPh 97-001 (1997).

9. G. PALMIOTTI et al., "VARIational Anisotropic Nodal Transport for Multidimensional Cartesian and Hexagonal Geometry Calculation", *Argonne National Laboratory Report, ANL-95/40* (1995).

10. S.PELLONI, E. Bubelis, K. Mikityuk, P. Coddington, "Calculations of Reactivity-initiated Transients in Gas-cooled Fast Reactors Using the Code System FAST", to be published in *Annals of Nuclear Energy*.

11. H. CHOI, G. Rimpault, and J.C. Bosq, "A Physics Study of a 600-MW(thermal) Gas-Cooled Fast Reactor", *Nuclear Science and Engineering*, **152**, 204–218 (2006).

12. D. DA CRUZ, A. Hogenbirk, J.C. Bosq, G. Rimpault, P. Morris, S. Pelloni, "Neutronic Benchmark on the 2400 MW Gas-cooled Fast Reactor Design", to be published in Proc. of PHYSOR-2006, Sept. 10-14, 2006, Vancouver, Canada (2006)

13. T. SHIMOO, H. Takeuchi, K. Okamura, "Thermal Stability of Polycarbosilane-Derived Silicon Carbide Fibers under Reduced Pressures", *J. Am. Ceram. Soc.*, **84**, 3, 566–70 (2001).

14. R.H. JONES et al., "Recent advances in the development of SiC/SiC as a fusion structural material", *Fusion Engineering and Design*, **41**, 15–24 (1998).